Research Article | Vol. 7, No. 11 | 1 Nov 2016 | BIOMEDICAL OPTICS EXPRESS 4416
Biomedical Optics EXPRESS

Fabrication and analysis of microfiber array platform for optogenetics with cellular resolution

JIAN-HONG CHEN,[1,4] MING-YI CHOU,[2,4] CHIEN-YUAN PAN,[2] AND LON A. WANG[3,*]

[1]*Graduate Institute of Photonics and Optoelectronics, National Taiwan University, Taipei, Taiwan*
[2]*Department of Life Science, National Taiwan University, Taipei, Taiwan*
[3]*Graduate Institute of Photonics and Optoelectronics, and Department of Electrical Engineering, National Taiwan University, Taipei, Taiwan*
[4]*These authors contributed equally to this work*
[*]*lon@ntu.edu.tw*

Abstract: Optogenetics has emerged as a revolutionary technology especially for neuroscience and has advanced continuously over the past decade. Conventional approaches for patterned *in vivo* optical illumination have a limitation on the implanted device size and achievable spatio-temporal resolution. In this work, we developed a fabrication process for a microfiber array platform. Arrayed poly(methyl methacrylate) (PMMA) microfibers were drawn from a polymer solution and packaged with polydimethylsiloxane (PDMS). The exposed end face of a packaged microfiber was tuned to have a size corresponding to a single cell. To demonstrate its capability for single cell optogenetics, HEK293T cells expressing channelrhodopsin-2 (ChR2) were cultured on the platform and excited with UV laser. We could then observe an elevation in the intracellular Ca^{2+} concentrations due to the influx of Ca^{2+} through the activated ChR2 into the cytosol. The statistical and simulation results indicate that the proposed microfiber array platform can be used for single cell optogenetic applications.

OCIS codes: (060.2280) Fiber design and fabrication; (170.2655) Functional monitoring and imaging; (250.5460) Polymer waveguides.

References and links

1. A. M. Aravanis, L. P. Wang, F. Zhang, L. A. Meltzer, M. Z. Mogri, M. B. Schneider, and K. Deisseroth, "An optical neural interface: In vivo control of rodent motor cortex with integrated fiberoptic and optogenetic technology," J. Neural Eng. **4**(3), S143–S156 (2007).
2. R. Pashaie, P. Anikeeva, J. H. Lee, R. Prakash, O. Yizhar, M. Prigge, D. Chander, T. J. Richner, and J. Williams, "Optogenetic brain interfaces," IEEE Rev. Biomed. Eng. **7**, 3–30 (2014).
3. J. Zhang, F. Laiwalla, J. A. Kim, H. Urabe, R. Van Wagenen, Y. K. Song, B. W. Connors, F. Zhang, K. Deisseroth, and A. V. Nurmikko, "Integrated device for optical stimulation and spatiotemporal electrical recording of neural activity in light-sensitized brain tissue," J. Neural Eng. **6**(5), 055007 (2009).
4. A. N. Zorzos, J. Scholvin, E. S. Boyden, and C. G. Fonstad, "Three-dimensional multiwaveguide probe array for light delivery to distributed brain circuits," Opt. Lett. **37**(23), 4841–4843 (2012).
5. T. V. F. Abaya, S. Blair, P. Tathireddy, L. Rieth, and F. Solzbacher, "A 3D glass optrode array for optical neural stimulation," Biomed. Opt. Express **3**(12), 3087–3104 (2012).
6. K. Y. Kwon, H. M. Lee, M. Ghovanloo, A. Weber, and W. Li, "Design, fabrication, and packaging of an integrated, wirelessly-powered optrode array for optogenetics application," Front. Syst. Neurosci. **9**, 69 (2015).
7. Y. LeChasseur, S. Dufour, G. Lavertu, C. Bories, M. Deschênes, R. Vallée, and Y. De Koninck, "A microprobe for parallel optical and electrical recordings from single neurons in vivo," Nat. Methods **8**(4), 319–325 (2011).
8. N. Grossman, V. Poher, M. S. Grubb, G. T. Kennedy, K. Nikolic, B. McGovern, R. Berlinguer Palmini, Z. Gong, E. M. Drakakis, M. A. A. Neil, M. D. Dawson, J. Burrone, and P. Degenaar, "Multi-site optical excitation using ChR2 and micro-LED array," J. Neural Eng. **7**(1), 016004 (2010).
9. S. Sakai, K. Ueno, T. Ishizuka, and H. Yawo, "Parallel and patterned optogenetic manipulation of neurons in the brain slice using a DMD-based projector," Neurosci. Res. **75**(1), 59–64 (2013).
10. B. K. Andrasfalvy, B. V. Zemelman, J. Tang, and A. Vaziri, "Two-photon single-cell optogenetic control of neuronal activity by sculpted light," Proc. Natl. Acad. Sci. U.S.A. **107**(26), 11981–11986 (2010).

#264869 http://dx.doi.org/10.1364/BOE.7.004416
Journal © 2016 Received 9 May 2016; revised 15 Jul 2016; accepted 22 Aug 2016; published 5 Oct 2016

Biomedical Optics EXPRESS

11. K. Dhakal, L. Gu, B. Black, and S. K. Mohanty, "Fiber-optic two-photon optogenetic stimulation," Opt. Lett. **38**(11), 1927–1929 (2013).
12. S. Satpathy, S. Batabyal, K. R. Dhakal, J. Lin, Y. T. Kim, and S. K. Mohanty, "Broad spectral excitation of opsin for enhanced stimulation of cells," Opt. Lett. **40**(11), 2465–2468 (2015).
13. A. Tripathi, P. Whittingstall, and G. H. McKinley, "Using filament stretching rheometry to predict standard formation and processability in adhesive and other non-Newtonian fluids," Rheol. Acta **39**(4), 321–337 (2000).
14. S. M. Berry, S. Pabba, J. Crest, S. D. Cambron, G. H. McKinley, R. W. Cohn, and R. S. Keynton, "Characterization and modeling of direct-write fabrication of microscale polymer fibers," Polymer (Guildf.) **52**(7), 1654–1661 (2011).
15. S. Dufour and Y. De Koninck, "Optrodes for combined optogenetics and electrophysiology in live animals," Neurophotonics **2**(3), 031205 (2015).
16. T. J. Foutz, R. L. Arlow, and C. C. McIntyre, "Theoretical principles underlying optical stimulation of a channelrhodopsin-2 positive pyramidal neuron," J. Neurophysiol. **107**(12), 3235–3245 (2012).
17. C. D. Mobley, "The optical properties of water." in *Handbook of Optics*, 2nd ed. (McGraw-Hill, 1995).
18. V. D. Tuan, *Biomedical Photonics Handbook: Biomedical Diagnostics* (CRC press, 2014).
19. F. Wu, E. Stark, M. Im, I. J. Cho, E. S. Yoon, G. Buzsáki, K. D. Wise, and E. Yoon, "An implantable neural probe with monolithically integrated dielectric waveguide and recording electrodes for optogenetics applications," J. Neural Eng. **10**(5), 056012 (2013).
20. K. Y. Kwon, A. Weber, and W. Li, "Varying-length polymer microneedle arrays fabricated by droplet backside exposure," J. Microelectromech. Syst. **23**(6), 1272–1280 (2014).
21. F. Zhang, L. P. Wang, E. S. Boyden, and K. Deisseroth, "Channelrhodopsin-2 and optical control of excitable cells," Nat. Methods **3**(10), 785–792 (2006).
22. D. T. Hartong, E. L. Berson, and T. P. Dryja, "Retinitis pigmentosa," Lancet **368**(9549), 1795–1809 (2006).
23. T. I. Kim, J. G. McCall, Y. H. Jung, X. Huang, E. R. Siuda, Y. Li, J. Song, Y. M. Song, H. A. Pao, R. H. Kim, C. Lu, S. D. Lee, I. S. Song, G. Shin, R. Al-Hasani, S. Kim, M. P. Tan, Y. Huang, F. G. Omenetto, J. A. Rogers, and M. R. Bruchas, "Injectable, cellular-scale optoelectronics with applications for wireless optogenetics," Science **340**(6129), 211–216 (2013).

1. Introduction

Optogenetics is a recently emerged photonics-based technology to manipulate cellular functions through the activation of light-sensitive proteins expressed in cells [1]. It potentially provides an alternative approach in understanding the neural circuit connections in the brain and in turn created a demand for optical devices that target delivery of light to subregions of the living brain. Various silicon-based microelectrodes have been developed to record neuronal signals or stimulate the nervous system as prosthetic devices. Optical neural stimulation based on optogenetics has several advantages over the conventional electrical stimulation; the stimulation could be noninvasive, permit activation or inhibition of specific types of neurons with sub-millisecond temporal control, and omit the electrical artifacts. In addition, multiple light-sensitive proteins with different excitation wavelengths can be expressed in a single cell so that the cell activities could be controlled with various colors of light.

Optogenetic brain/machine interfaces have been developed to control the distribution of light inside the brain and even combined with other stimulation or imaging modalities such as electrophysiology, electrocorticography, nonlinear microscopy, and functional magnetic resonance imaging [2]. The optical properties of tissues limit the penetration depth of visible light; henceforth, optogenetic tools to guide light delivery for *in vivo* applications are developed rapidly [3]. In the past few years, a lot of efforts have been spent to design optogenetic probes in a dual optical and electrical way with high temporal and spatial resolution for *in vivo* applications. A new class of devices capable of delivering patterned light into different regions of brain based on SiON, glass, or SU8 resist waveguide in optrode array mode have been developed [4–6]. Short term *in vivo* optical experiments have been conducted in mouse model, however, resist waveguide could be degraded with continuous exposure to blue light in long term experiment [6]. In contrast, optogenetic stimulation with single cell resolution using laser or light-emitting diode (LED) coupled fiber taper [7], micro LED array [8], digital micro mirror device (DMD)-based projector through a microscope [9], two-photon temporal focusing [10], etc, have also been developed. Silica fiber taper is the most common approach to illuminate light at the designate regions of brain. To achieve the

Biomedical Optics EXPRESS

dual capability of optical delivery and electrical recording, a fiber taper-based optrode has been developed [3]. Metal coating on fiber taper could not only provide electrical recording capability but also confine the spot size in emitting light. Recently, a microprobe for simultaneous optical and electrical recordings has been demonstrated for single cell optogenetics [7]. To achieve patterned optical stimulation, a tapered fiber array must be a long penetrating device resulting in unavoidable damages to the brain tissue during implantation [5]. A micro-LED array could generate arbitrary optical excitation patterns on a neuronal sample with micrometer and millisecond resolution [8]; however, the spatial resolution was limited by the Lambertian emission profile of the micro LED. Microscope equipped with DMD-based projector or two-photon excitation system could elevate the spatial resolution to single-cell level and even have the excitation in 3-D pattern [9,10]; however, the associated microscope objective and pulsed light source limit the applications. Among those developed single cell optical neural stimulation methods, silica fiber taper could not be the optimal solution of chronic implants due to the damage in implantation. Resist material based waveguide could minimize implantation damage but could be degraded under blue light in long term experiment. The emission profile and material compatibility limits the *in vivo* optogenetic applications of micro LED with high cellular resolution.

In this work, in view of the geometry of silica fiber taper and high biocompatibility, low Young's modulas, simple fabrication and shaping process properties of Poly(methyl methacrylate) (PMMA), we proposed that a flat PMMA-based waveguide array with tapering geometry could be implanted in certain depth of tissue without penetrating it. The disadvantages of resist material and silica taper in chronic implantation applications could be minimized [5,6]. We developed a novel fabrication process to produce a microfiber array platform which has an illumination capability for single-cell optogenetic stimulation as a step toward future chronic *in vivo* applications. PMMA and polydimethylsiloxane (PDMS) with different refractive indices were served as the core and cladding of the microfiber array, respectively. The advantages of fabricating microfibers with PMMA and packaged with PDMS include high transparency in wavelengths of visible light, high flexibility, high biocompatibility, and low tissue damage for long-term implant applications. To evaluate the microscale optical stimulation capability on microfiber array, we cultured HEK293T cells expressing channelrhodopsin 2 fused with a mCherry fluorescent protein at the C-terminal (ChR2m) on the microplate and examined the changes in the intracellular Ca^{2+} concentration ($[Ca^{2+}]_i$) upon optogenetic excitation [11,12]. The results revealed that HEK293T expressing ChR2m had a significant elevation in $[Ca^{2+}]_i$ when compared to the control cells. Along with optical simulation results, our system could be used for single cell optogenetic applications.

2. Materials and methods

2.1 Fabrication of microfiber array

Microfiber array was drawn with PDMS micro rods from a PMMA homopolymer (996 kDa, Sigma-Aldrich) solution (23% in chlorobenzene). The diameter and spacing of PDMS micro rods were chosen as 100 μm and 500 μm, respectively. To fabricate the PDMS micro rods, hole arrays were fabricated by employing lithographical process with SU8 photoresist. PDMS (Sylgard 184, A: B = 10: 1 w/w) was prepared, degassed and poured on the SU8 hole arrays and cured at 100 °C for 60 min. After fully cured, the PDMS micro rods was peeled off from the SU8 mold. Thin metal layer was sputtered on the PDMS micro rods to modify the surface property before serving as a drawing agent while maintaining its optical transparency for the observation of cellular fluorescence activities.

Fabrication steps of microfiber array platform is shown in Fig. 1. The arrayed fiber drawing system was built on a linear translation stage to control manually or electrically the distance between the PDMS and PMMA thin film plates. In Fig. 1(a), the PDMS micro rods were first mounted on the linear translation stage and then approached to the spin coated PMMA thin film on a 0.12-mm thick silica plate. To draw PMMA microfiber taper, the

Biomedical Optics EXPRESS

typical spin coating parameter was 3000 rpm for 16 seconds in a standard clean room and the thickness of the PMMA thin film coating was about 20 μm for 23% PMMA/chlorobenzene solution after solidification. If the spin time was too long (> 20 sec), the prepared thin film solidified, while if too short (< 10 sec), the PDMS micro rods couldn't draw any micro fiber. Once attached to each other, the PDMS micro rods were moved in an opposite direction and the arrayed microfiber were drawn between the PDMS and PMMA thin film plates shown in Fig. 1(b). During fiber drawing process, the initial and final diameters of a single fiber can be expressed by

$$D(t=\infty) = D_1 e^{-0.0709/2P} \quad (1)$$

where D_1 is the initial fiber diameter, D the final fiber diameter, the processability parameter $P = \eta\chi / \sigma$, which combines the influence of viscosity η, solvent evaporation rate χ and surface tension σ. Equation (1) is valid when $P \neq 0$, and in the limit when $P = 0$ the micro fiber would be drawn broken [13]. Compared with the direct-write fabrication of single polymer micro fiber [14], the capillary thinning process of each micro fiber in the dense array was affected by the vapor concentration of chlorobenzene during the solidification of micro fibers. As long as the local vapor concentration in the array space continued increasing, the solvent evaporation rate χ of some micro fibers became zero, so did the processability parameter. Some microfibers were drawn to broken. Thus, A DC fan (Sunon Fans, PMD1212PMB1-A) with air flow 190 CFM (5.38 m^3/min) at 12V was utilized to produce steady air flow in the drawing process to modify the tapering profile of microfiber. First, the PMMA microfiber array was drawn manually on a linear translation stage to form a varying biconical taper profile slowly under steady air flow produced by a DC fan at 12V. Then it was drawn electrically to form a rapidly varying taper profile under smaller air flow produced by a DC fan at 6V. The drawn microfiber taper was in the diameter of several micrometers and the whole PMMA microfiber array could be easily torn apart from the PMMA thin film after solidification.

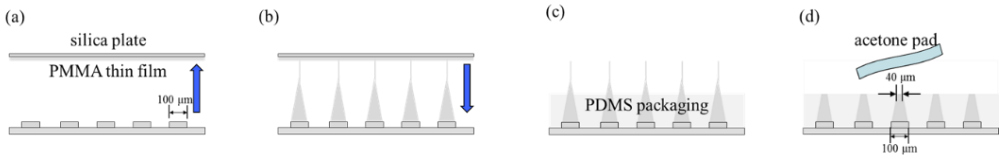

Fig. 1. (a)-(d). Fabrication steps of microfiber array platform.

2.2 Packaging of microfiber array

The PMMA microfibers drawn on PDMS micro rods was glued on the plastic dish. The packing material was chosen as PDMS, which is biocompatible and low absorption in the visible light. Due to the low Young's modulas of PMMA microfiber, we diluted uncured PDMS (Sylgard 184, A: B = 10: 1 w/w) with Hexane (10: 1 w/w) to prevent microfiber from bending or collapsing during packaging process. It was mixed and degassed then poured into the dish. The surface intersected with PMMA microfiber was monitored under optical microscope and it defined the diameter of exposed microfiber end face. Then, the dish was heated to 70°C for 12 hours for the total cure of PDMS shown in Fig. 1(c). Then the unpackaged microfiber tapers were manually removed with acetone pad. The exposed end face of packaged microfiber was controlled to be in a diameter similar to the size of a HEK293T cell as shown in Fig. 1(d). The calculated numerical aperture of packaged PMMA microfiber was 0.48 according to the refractive index of the PMMA core and PDMS cladding material at 405 nm. The acceptance or irradiance angle (θ_a) of packaged PMMA microfiber in water was 7.38°.

Biomedical Optics EXPRESS

2.3 Simulation of irradiance profile

The irradiance profile in diffuse scattering media was simulated from a simplified MATLAB script by Dufour et al. based on the model described by Foutz et al [15,16]. The radius of microfiber and numerical aperture were set as 17.5 μm and 0.48, respectively. The refractive index of water at 405 nm is 1.34. The values of absorption and scattering coefficients (K, S) of water at 400 nm are 0.018 m^{-1} and 58.1 m^{-1}, respectively [17]. The refractive index of typical brain tissue at 400 nm is 1.36. The values of absorption and scattering coefficients (K, S) of typical brain tissue at 400 nm are 2.6 cm^{-1} and 128.5 cm^{-1} [18]. Figure 2(a), 2(b) showed simulated two-dimensional representation of irradiance profiles in water and tissue environments. Normalized intensity profiles in water and tissue environments at different axial distances were shown in Fig. 2(c), 2(d). The calculated full width at half maximum (FWHM) increased from 10 μm at microfiber end face to 21 μm at axial distance of 50 μm both in water and tissue environments. The axial irradiance profile at microfiber center shown in Fig. 2(e) decayed to its half magnitude in axial distance of over 25 μm in tissue and 46 μm in water environments. From the simulation results shown in Fig. 2(c)-2(e), the irradiance profile on microfiber shows an axial resolution of 25 μm in tissue and 46 μm in water environments. The transverse resolution in both environments was 10 μm which was smaller than the size of a HEK293T cell and thus could reach subcellular spatial resolution for optogenetics. For *in vivo* applications, the axial resolution in tissue could be smaller than 10 μm with smaller diameter of microfiber to confine the optical excitation at the first layer of neurons.

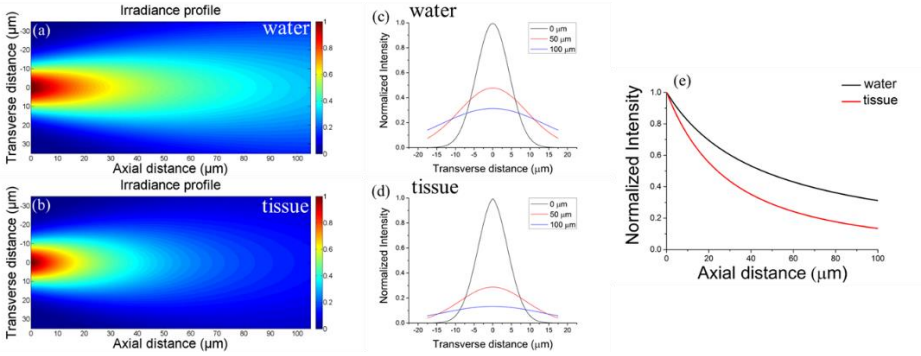

Fig. 2. Simulated irradiance profiles. (a, b) The simulated irradiance profile on the end face of microfiber platform in (a) water and (b) tissue environments. (c, d) Normalized intensity profile at axial distance of 0, 50, 100 μm in (c) water and (d) tissue environments. (e) Axial normalized intensity profile at microfiber center.

2.4 Cell culture and transfection

HEK293T cells were transfected with ChR2(H134R)-mCherry (ChR2m) construct using Lipofectamine LTX according to the manufacturer's instructions. Two days after transfection, the cells were resuspended and seeded on the microfiber array platform coated with 10 μg/ml fibronectin (Sigma-Aldrich) for 1 h at room temperature for cell adhesion. The cells were washed with Hank's balanced salt solution (HBSS) three times and then incubated in HBSS containing Fluo-2 MA AM (0.5 μM, TefLabs, Austin, TX, USA) at 37°C in a 5% CO_2 humidified atmosphere for 40 minutes. The cells were washed three times with HBSS before conducting the experiments. The bath solution was (in mM): 150 NaCl, 5 glucose, 5 KCl, 1 $MgCl_2$, 2.2 $CaCl_2$, and 10 HEPES, pH 7.3 with NaOH (300 mosm/kg).

Biomedical Optics EXPRESS

2.5 Optogenetic activation of single cells

The The experimental setup for optogenetic activation of single cells on microfiber array platform was shown in Fig. 3. The microplate with cells was plated at the stage of an inverted Nikon TiE microscope and the cells expressing ChR2m were verified by the mCherry fluorescence. The cells were illuminated with a 405-nm laser provided by a Mosaic system (Andor Technology plc., Belfast, UK) through a 40 × objective to activate the ChR2m and the $[Ca^{2+}]_i$ was examined by the changes in the fluorescence intensity of Fluo-2. Although the sensitivity of ChR2 to violet (405 nm) versus blue (470 nm) light source is approximately 60%, we chose violet rather than blue light to excite ChR2m to avoid the interference from Fluo 2 whose absorption maxima is at about 490 nm [19]. The excitations for Fluo 2 and mCherry were provided by DG-4 (Sutter Instrument, CA, USA) with appropriate filter cubes; the emission images were captured with a CCD camera (eVolve 512, Photometrics Technology Inc., Tucson, AZ, USA). The whole system was controlled by NIS Element software (Nikon). The change in the fluorescence intensity of Fluo 2 (ΔF) was determined by the difference between the averaged fluorescence intensity in 10 seconds before laser illumination (F_0) and the highest fluorescence intensity after illumination. Curve fitting and statistical analysis was performed using Origin Software (Origin Lab Corp., Northampton, MA). Data are presented as mean ± SEM and analyzed using a Student's paired *t* test. A value of $p < 0.05$ was considered to be statistically significant.

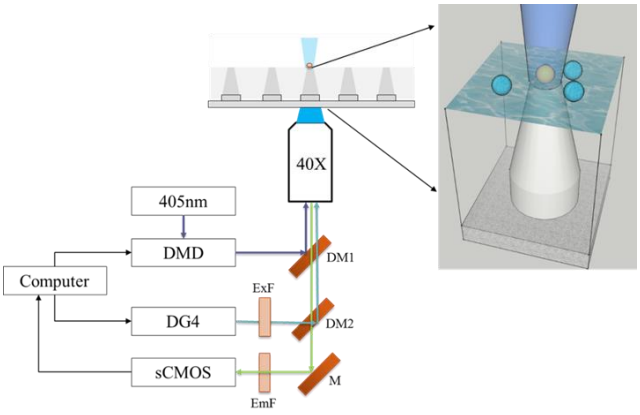

Fig. 3. Experimental setup for optogenetic activation of single cells on microfiber array platform.

3. Results and discussion

3.1 The fabricated microfiber array platform and its optical characteristics

The top view of optical microscope image of PDMS micro rods is shown in Fig. 4(a). The array has a size of 2 × 2 mm^2 containing 3 × 3 individual waveguides. We could also produce arrays of larger size with 10 × 10 waveguides drawn simultaneously. The SEM image (Fig. 4(b)) showed that each PMMA microfiber exhibited an identical tapering profile in the 4 × 4 array and the side view image acquired by an optical microscope was shown in Fig. 4(c). After PDMS packaging, the unpackaged microfiber tapers were manually removed with an acetone pad. The top view of the packaged microfiber array showed that the exposed end surface had a diameter of about 40 μm (Fig. 4(d)). To characterize the light transmission property, black PDMS (Sylgard 170, A: B = 1: 1 w/w) was chosen as the packaging material and the packaged PMMA microfiber platform was illuminated from the bottom with a blue LED light source. The exposed microfiber end face was enlightened as shown in Fig. 5(a). The intensity of the three light spots in the middle row (Fig. 5(b)) revealed an evenly

Biomedical Optics EXPRESS

distributed light intensity on the end faces of packaged PMMA microfibers and the average and standard deviation of FWHM of the 9 light spots was 40.3 ± 1.9μm. To observe the light propagation in scattering media, gelatin (20% w/w) was prepared and covered on the end face of microfiber [20]. The measured light spot when fitted with Gaussian had a FWHM of 18.4 μm, which is 46% of that in air environment (Fig. 5(c)).

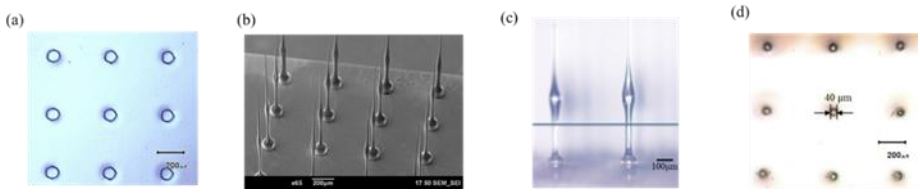

Fig. 4. (a) The top view of optical microscope image of PDMS micro rods. (b) SEM image of drawn microfibers. (c) The side view of optical microscope image of drawn PMMA microfibers. The blue line indicates the packaged PDMS plane. (d) The top view of optical microscope image of exposed end face of packaged microfiber array.

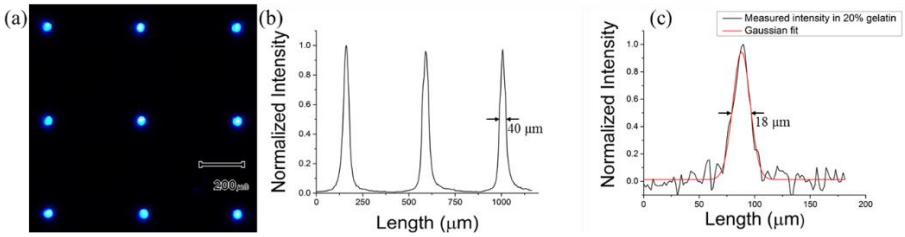

Fig. 5. (a) The optical microscope image of blue light spots on black PDMS packaged microfiber array illuminated by blue LED. (b) Measured intensity of the blue LED light emission on the microfiber array in the middle row. (c) Measured intensity of light emission on the end face of microfiber through gelatin (20% w/w).

3.2 Cell imaging and measurement of $[Ca^{2+}]_i$

To verify the excitation light guided through the platform could activate the ChR2m expressed in the attached HEK293T cells, we loaded the cells with a Ca^{2+}-sensitive fluorescence dye to monitor the changes in the $[Ca^{2+}]_i$ ($\Delta F/F_0$). The cells on the platform could be observed through the transparent PMMA and PDMS by visible light (Fig. 6(a)). The microscope was then tuned to observed the mCherry fluorescence to located the cells expressing ChR2m (Fig. 6(b)). The entire imaging field was illuminated with a 405-nm laser (100 ms pulse, on/off ratio = 1:1, 1 sec duration) with an intensity of about 0.84 μW/μm^2 on the packaged microfiber end face to activate the ChR2m. Because of the low excitation efficiency of ChR2m at 405 nm, the power applied was an order of magnitude higher than using 470 nm light [21].

Since the ChR2m-conjugated ion channel has a permeability for Ca^{2+}, we monitored the $[Ca^{2+}]_i$ elevation by a Ca^{2+}-sensitive fluorescence indicator. The imaging (broadband white light source) vs ChR2 (405nm laser) activation intensity ratio in experiment was about 1:7. A control experiment (not shown) showed that the imaging light would not cause a depolarization on HEK cells without ChR2 expression during experiment. The representative fluorescence traces of cells expressing ChR2m, but not control plasmid, showed an elevation in the intensity (Fig. 6(c), 6(d)). The average $[Ca^{2+}]_i$ changes were significantly increased from 0.02 ± 0.002 (n = 10) of control group to 0.24 ± 0.07 (n = 11) of cells expressing ChR2m ($p < 0.005$) (Fig. 6(e)). These data suggest that our platform could successfully guide the light to activate the ChR2 expressed in the cells located at the surface of the endings.

Biomedical Optics EXPRESS

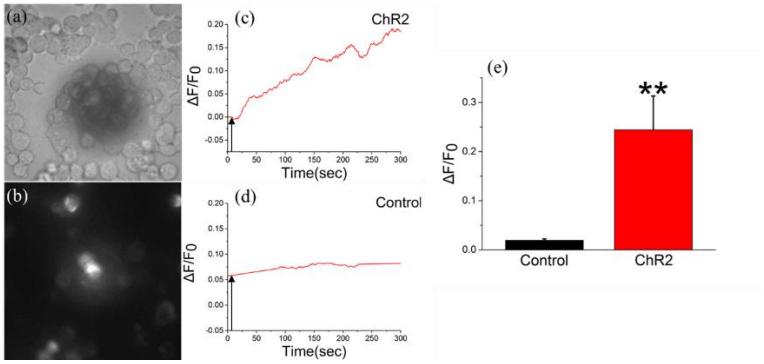

Fig. 6. Optogenetic stimulation of single HEK293T cell. (a) Bright field and (b) mCherry fluorescence images of cultured HEK293T cells seeded on the end face of the microfiber platform. (c, d) Representative fluorescence intensity traces of a Ca^{2+} sensitive dye from HEK293T cells expressing (c) ChR2m or (d) a control plasmid. The arrow indicated the application of a 405-nm laser. (e) The average changes in the fluorescence intensity of the Ca^{2+}-sensitive dye in cells after UV illumination. The sample number for cells expressing ChR2m or a control plasmid were 11 and 10, respectively. Data presented were Mean ± S.E.M; **: $p < 0.005$ when compared with the control group.

4. Conclusion

A highly biocompatible microfiber array has been fabricated using lithography-based fabrication technology. It has the advantages of low cost, simple fabrication, and flexible thin film structure. PMMA and PDMS with different refractive indices can serve as the core and the cladding of the microfiber array, respectively, with high transparency in wavelengths of UV-to-visible light for optogenetic applications. In addition, the microfiber array can be potentially integrated with transparent thin film microelectrodes, allowing light evoked cellular activities to be simultaneously recorded using the same alignment.

We have also demonstrated the capability of this microfiber array in guiding the UV laser to photoactivate the ChR2 expressed on single HEK293T cells. When integrated this device with a micro LED array, the platform is expected to offer a patterned multicolor optical stimulation for *in vivo* clinical applications on nervous system such as visual prosthetic device to restore physiological functions after loss of vision from retinitis pigmentosa [22]. For micro LED to couple light to PDMS microrod in the diameter of 100 μm, the efficiency of butt coupling could be over 80% [20]. To meet the requirement of output light intensity (1 mW/mm^2) at wavelengths near 450nm for many optogenetic constructs [23], the input light intensity could be calculated according to the butt coupling efficiency of micro LED (~80%) and the transmission loss of PMMA microfiber (~50%). The miniaturization of the device to be implanted for wireless optogenetics should take into account the generated heat of micro LEDs to meet the safety protocol.

Funding

This work was supported in part by the National Taiwan University through the International Collaboration Project under Grant NTU-ICRP-104R7558 and in part by the Ministry of Science and Technology under Grant 101-2221-E-002-079-MY2 and Grant 103-2221-E-054-MY3.